Comparison of Tip-Tilt Controllers using the STRAP Wavefront Sensor in the W.M. Keck Observatory Laser Guide Star Adaptive Optics System

Douglas P. Looze[a,*], Marcos A. van Dam[b,**] and Erik M. Johansson[b,***]

[a]Dept. of Electrical and Computer Engineering, University of Massachusetts, Amherst, MA 01002

[b] W. M. Keck Observatory, 65-1120 Mamalahoa Highway, Kamuela, HI 96743

ABSTRACT

The W. M. Keck Observatory adaptive optics (AO) system uses the STRAP wavefront sensor to sense tip-tilt using a natural guidestar. The higher-order wavefront sensing can be done using light from either a laser guidestar (LGS) or a natural guidestar (NGS). The tip-tilt guidestar can be as bright as 10th or as faint as 19th magnitude. In both cases, as high a control bandwidth as possible is desired. Thus, it is of interest to determine the potential of various control algorithms over a wide range of signal-to-noise ratios (SNRs).

This paper compares two control algorithms using a set of tip-tilt data taken with the STRAP wavefront sensor (a set of four avalanche diodes arranged as a quad cell). The two algorithms are the standard integral control and a minimum variance (LQG) control designed using the power spectral density (PSD) of the data. The bandwidths of the integral control and the minimum variance control are adjusted to produce the least RMS residual wavefront error. The controllers are compared for SNRs representative of the expected range of guidestars.

1. INTRODUCTION

The purpose of this paper is to compare the performance of control algorithms for the tip-tilt (TT) loop of adaptive optics (AO) systems using data from the TT wavefront sensor at the W. M. Keck Observatory. Laser Guide Star (LGS) AO[1] systems require the use of a natural guide star to elicit tip and tilt information that is not available from the laser target. In addition, having a separate tip-tilt loop can improve the performance of NGS AO systems as well, since a single quad cell is more sensitive to tip-tilt than a Shack-Hartmann wavefront sensor.

The W. M. Keck Observatory LGS AO system[2,3] uses STRAP as the TT sensor. STRAP (System for Tip-tilt Removal using Avalanche Photodiodes) is an integrated unit manufactured by Microgate. The sensing is done with a quad cell of avalanche photodiodes. The centroid is then calculated, converted to mirror space and then passed through a third-order controller with configurable coefficients. It is operated with both bright guidestars and with guidestars as faint as 19th magnitude. In both cases, as high a control bandwidth as possible is desired. Thus, it is of interest to determine the potential of various control algorithms over a wide range of signal-to-noise ratios (SNRs).

This paper compares two control algorithms using a set of tip-tilt data taken with the STRAP wavefront sensor (a set of four avalanche diodes arranged as a quad cell). The two algorithms are the standard integral control[4] and a minimum variance (LQG) control[5] designed using the power spectral density (PSD) of the data. The primary comparison will be the residual RMS (square root of the variance). However, Bode magnitude plots of the loop transfer function and rejection transfer function, the loop bandwidth, and the stability margins of both designs will also be compared.

The objective of this comparison is to determine the peak performance that can be achieved by each compensator. Thus, the same data will be used to tune and evaluate the performance of the compensators. The bandwidths of the integral control and the minimum variance control will be adjusted to produce the least RMS residual wavefront error.

* Email: looze@ecs.umass.edu
** Email: mvandam@keck.hawaii.edu
*** Email: erikj@keck.hawaii.edu

2. TIP-TILT SYSTEM WITH STRAP MEASUREMENTS

2.1 Sampled-Data Feedback System

The STRAP tip-tilt system estimates the tip and tilt modal coefficients from a measurement of the wavefront produced by a natural guidestar, and uses this estimate to drive the actuators of a tip-tilt mirror. Its objective is to minimize the contribution by these modes to the steady-state variance (averaged over the pupil) of the residual wavefront phase. The architecture of the STRAP feedback loop is shown in Figure 1. An incident wavefront $\mathbf{w}(t)$ is reflected off a tip-tilt mirror which introduces a wavefront, $\mathbf{s}_m(t)$, to produce the residual wavefront

$$\mathbf{e}(t) = \mathbf{w}(t) - \mathbf{s}_m(t) \tag{1}$$

The residual wavefront is sensed by 4 avalanche photodiodes (APDs) operating at frame rate f_S (frame period $T_S = 1/f_S$), from which the modal coefficients $\hat{\mathbf{m}}_k$ of tip and tilt are reconstructed by the normalized (by the sum of the APD counts) reconstruction matrix $\mathbf{R}$

$$\mathbf{R} = \frac{1}{r}\begin{bmatrix} 1 & -1 & -1 & 1 \\ -1 & -1 & 1 & 1 \end{bmatrix} \tag{2}$$

Although not shown in Figure 1, the resulting raw centroids are rotated to give centroid measurements that are aligned with the mirror coordinates. The estimates of the modal coefficients are corrupted by measurement noise $\boldsymbol{\theta}_k$ [*] to produce the compensator measurement $\mathbf{y}_k$. This signal is processed by the compensator to produce the discrete-time mirror commands $\mathbf{a}_k$, which are input to a zero-order hold (ZOH) that uses the same frame rate f_S as the APDs. The outputs of the ZOH are the continuous-time mirror commands, which are applied to the tip-tilt mirror to produce the mirror attitude. The mirror is modeled as having identical, linear dynamics with transfer function $G(s)$ in both the tip and tilt loops. The computational loop delay is assumed to be τ s.

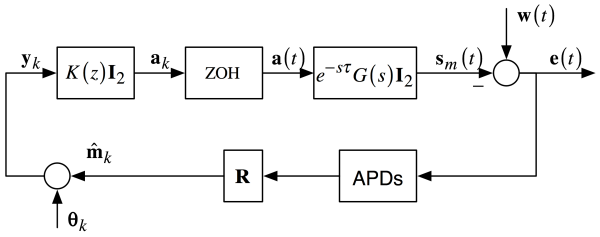

Figure 1. The STRAP tip-tilt adaptive optics system.

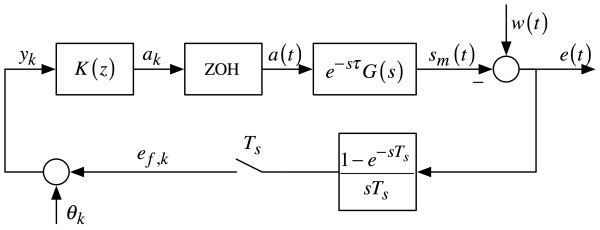

Figure 2. The STRAP feedback loop decouples into independent scalar feedback loops for each of the tip and tilt modes.

It will be assumed that in the absence of measurement error the tip and tilt modes that are present in the residual wavefront are reproduced exactly by the APD measurement followed by the reconstruction (i.e., the components of $\hat{\mathbf{m}}_k$ are the tip and tilt modal coefficients of the residual scaled by the centroid gain). Then, because the tip and tilt Zernike modes are uncorrelated and all transfer functions in Figure 1 are identical in each mode, the STRAP system shown in Figure 1 can be modeled as two identical scalar feedback systems (one each for tip and tilt) as shown in Figure 2.

In Figure 2, the disturbance vector $w(t)$ is the modal coefficient of the incident wavefront $\mathbf{w}(t)$ in Figure 1 of the tilt (or tip) mode. The output of the APDs and reconstruction are modeled by the sample values of the integration of the

[*] The output voltages of the APDs are actually subject to measurement noise. However, if the noise processes in all 4 measurements are white and independent with identical PSDs, the orthogonally of the rows of **R** (2) implies that the measurement noise can be modeled as in Figure 1 with the elements of $\boldsymbol{\theta}_k$ independent white noise processes.

residual of this mode over one frame. The equivalent objective is to minimize the temporal steady-state variance of the residual:

$$\sigma^2 = \lim_{\bar{T}\to\infty} \frac{1}{\bar{T}} \int_0^{\bar{T}} e^2(t)\,dt \tag{3}$$

2.2 Digital Feedback System

The feedback system shown in Figure 2 is a sampled-data feedback system involving both continuous-time and discrete-time signals. The system in Figure 2 can be represented in discrete-time by the system shown in Figure 3. The discrete-time transfer function model $G(z)$ incorporates the effects of the mirror dynamic model, the loop delay, the ZOH, the frame integration and sampling of the APDs, and the reconstruction. It can be computed using the algorithm in reference[7].

The values at the sample times of the frame-integrated residual sequence $e_{f,k}$ in the discrete-time feedback system (indicated by the subscript *f*) in Figure 3 are the same as the values of the corresponding sequence $e_{f,k}$ in Figure 2. The sequence is zero mean with variance identical to the residual variance of $e(t)$ [5]:

$$\sigma_f^2 = \lim_{L\to\infty} \frac{1}{L} \sum_{k=0}^{L} e_{f,k}^2 = \sigma^2 \tag{4}$$

Thus, the variance of the frame-integrated residual in Figure 3 is the residual variance to be minimized.

3. TIP-TILT COMPENSATORS

3.1 Procedure for Comparison

The performance of two controllers – the integral compensation that is typically used in adaptive optics loops[4] and the minimum variance controller[5] – will be compared on data obtained from the Keck STRAP TT controller. The design of each compensator will be optimized for the data set on which it is evaluated to compare the best possible performance of the compensators.

The TT mirror is modeled by the continuous-time transfer function:

$$G(s) = \frac{8.52\times10^{10}}{s^3 + 1.32\times10^4 s^2 + 5.808\times10^7 s + 8.52\times10^{10}} \quad \tau = 0 \tag{5}$$

Closed-loop APD outputs from a 10th magnitude star were gathered by the STRAP measurement system operating at a frame rate of 1 kHz. The transfer function of the compensator used to gather the closed-loop data was

$$K(z) = \frac{0.05z}{z-1} \tag{6}$$

The tip and tilt modal coefficients were reconstructed from this data using Eq. (2), and the PSDs of each signal were estimated using Welch's method[6]. The Euclidean norm of closed-loop the tip and tilt PSDs was computed and the result divided by the square of the norm of the rejection transfer function computed using Eqs. (5) and (6). The measurement noise PSD was estimated as average of the last 10% of the points of this PSD (frequencies above 450 Hz) and subtracted from the estimated PSD. The resulting PSD will be used to represent the "truth" statistics of the disturbance and is shown in Figure 4.

The effect of different guidestar brightness will be modeled as additional measurement noise (reflecting different values of the APD counts in one frame). Thus, the measurement noise PSD for a 10th magnitude star is modeled as a constant

3.8×10^{-5} (APD count 3×10^{6}, see Figure 4), for a 15th magnitude star is modeled as a constant 4.0×10^{-3} (APD count 3×10^{4}), and for a 18th magnitude star is modeled as a constant 6.8×10^{-2} (APD count 3×10^{3}).

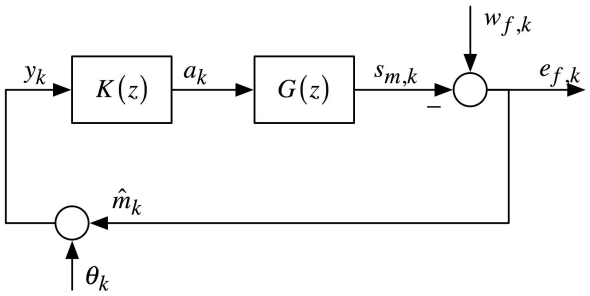

Figure 3. Representation of the STRAP feedback system as a discrete-time feedback system. The discrete-time transfer function $G(z)$ incorporates the effects of the mirror dynamic model, the loop delay, the ZOH, the frame integration and sampling of the APDs, and the reconstruction.

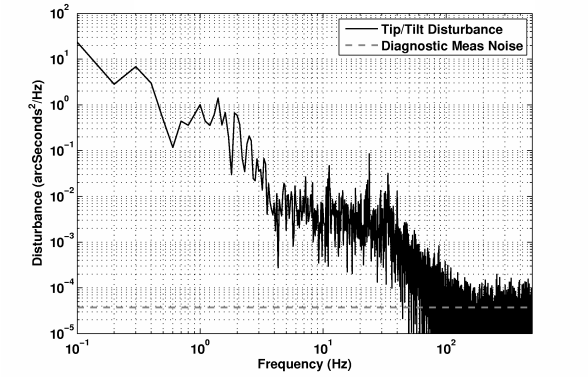

Figure 4. PSD of atmospheric tip-tilt disturbance to be used as "truth" model for evaluation.

The residual variance will be computed using the discrete-time model of the adaptive optics system (Figure 3) with the STRAP mirror model given in continuous-time by Eq. (5). The discrete-time transfer function computed with[7] is:

$$G(z)=\frac{3.782\times10^{-4}z^3+5.501\times10^{-4}z^2+3.532\times10^{-5}z+1.298\times10^{-7}}{z^4-3.673\times10^{-2}z^3+4.534\times10^{-4}z^2-1.851\times10^{-6}z} \tag{7}$$

3.2 Compensators

3.2.1 Integral Compensation

The base compensator is an integral compensator that is typically used in adaptive optics loops:

$$K(z)=K_I(z)=g\frac{z}{z-1} \tag{8}$$

The gain g is selected based on the measurement noise PSD and the disturbance PSD (Figure 4) to minimize the residual variance. The minimization procedure used to determine the gain is a golden section search[8] with a tolerance of 10^{-3} nm.

As shown in reference[5], the minimum variance compensator is an integral compensator when the mirror has no dynamics, the loop delay is zero, and the PSD of the disturbance is proportional to f^{-2}. The addition of actuator lags to the mirror model or computational loop delay result in the integral compensator in Eq. (8) being modified by adding lead filters. The amount of lead is determined by the actuator time constant and delays[5]. A model of the disturbance PSD is incorporated in the minimum variance controller structure. Thus, the integral compensator Eq. (8) can be regarded as being a minimum variance compensator for a particular model (f^{-2}) of the PSD of the aberration (with no mirror dynamics or delay). When the disturbance PSD is modified from the f^{-2} behavior inherent to the integral controller, the controller dynamics are modified accordingly.

3.2.2 Minimum Variance Compensation

The minimum variance compensator[5] is the solution of a linear-quadratic-Gaussian (LQG) steady-state optimization that uses the steady-state residual variance Eq. (4) as its objective. The mirror dynamics and disturbance are modeled using the discrete-time transfer functions to produce a discrete-time feedback system as shown in Figure 3.

The discrete-time model used for the LQG formulation incorporates the ZOH, the loop delay, continuous-time mirror dynamics, and the WFS in a single discrete-time transfer function. Although the mirror can be modeled with no delay and continuous-time dynamics (see Eq. (5)), the resulting controller has dynamic order greater than what can currently be implemented on the STRAP system. Instead, the LQG model will be based on the transfer function of a stiff mirror ($G(s)=1$) and a non-zero delay. Figure 5 shows that a delay of 0.6 frames (0.0006 s) gives a discrete-time transfer function that is a good approximation of the identified mirror model.

The LQG formulation assumes that the discrete-time disturbance $w_{f,k}$ is the output of a linear "coloring" filter with a discrete-time white noise input d_k (see Figure 6). The PSD of the disturbance is:

$$\mathbf{\Phi}_w(f)=\left|G_a\left(e^{j2\pi T_s f}\right)\right|^2 \tag{9}$$

Thus, the PSD of the measured sequence (Figure 4) can be approximated by specifying the magnitude of the transfer function $G_a(z)$ appropriately.

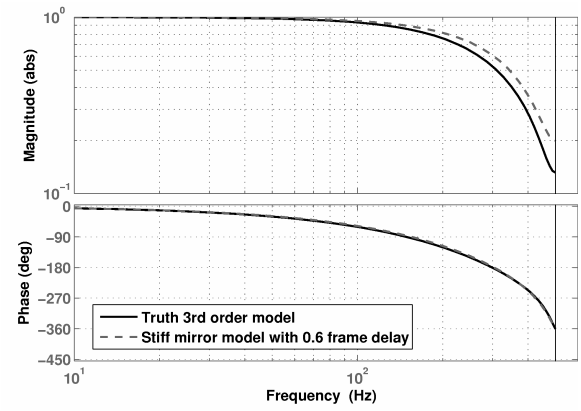

Figure 5. Comparison of discrete-time equivalent of the identified mirror model Eq. (7) and the discrete-time equivalent of a stiff mirror with 0.6 frame delay.

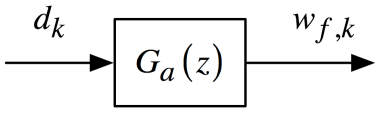

Figure 6. The disturbance sequence is generated by a linear system whose input d_k is a unit PSD white noise sequence.

As with the mirror model in the LQG formulation, a higher-order coloring filter will lead to a higher order controller. The PSD of the measured disturbance Figure 4 will be approximated by a 2nd order coloring filter:

$$G_a(z)=g_a\left(\frac{z+1}{z-1}\right)\left(\frac{z-\beta}{z-\alpha}\right) \tag{10}$$

A good approximation to the measured PSD is obtained for

$$\begin{aligned}\alpha &= 0.957 \qquad (7\text{ Hz corner frequency})\\ \beta &= 0.975 \qquad (4\text{ Hz corner frequency})\end{aligned} \tag{11}$$

Figure 7 shows the measured disturbance PSD (from Figure 4) and the PSD of the modeled disturbance for $g=0.01$. In general, the resulting minimum variance compensator will depend on the level of the magnitude g of the coloring

filter Eq. (10). As for the integral controller, this magnitude will be selected to minimize the residual variance of the design.

4. COMPARISON OF PERFORMANCE

The performance of the two controllers will be compared for 10^{th} magnitude (bright), 15^{th} magnitude (medium) and 18^{th} magnitude (faint) guidestars. The primary comparison will be the residual RMS (square root of the variance). However, Bode magnitude plots of the loop transfer function and rejection transfer function, the loop bandwidth, and the stability margins of both designs will also be compared.

4.1 Bright Guidestar

Table 1. Performance using a bright guidestar.

	Integral Controller	**Minimum Variance Controller**
Residual RMS	100.5 nm	92.4 nm
Rejection Bandwidth	53 Hz	74 Hz
Phase Margin	72.5˚	83.3˚

The minimum variance compensator produces an 8.1% smaller residual variance than the integral compensator (see Table 1). The integral compensator that produces the minimum residual RMS is:

$$K_I(z) = 0.261\frac{z}{z-1} \tag{12}$$

The minimum variance compensator uses a disturbance model given by Eq. (11). The coloring filter gain that result in a minimum residual RMS is $g_a = 0.0121$ (see Figure 7). The resulting minimum variance compensator is:

$$K_{MV}(z) = 0.5\left(\frac{z}{z-1}\right)\left(\frac{z}{z+0.95}\right)\left(\frac{z-0.975}{z-0.957}\right) \tag{13}$$

Note that the minimum variance compensator consists of an integral element with two lead filters. One lead filter incorporates the model of the disturbance. The other lead filter compensates for the loop delay.

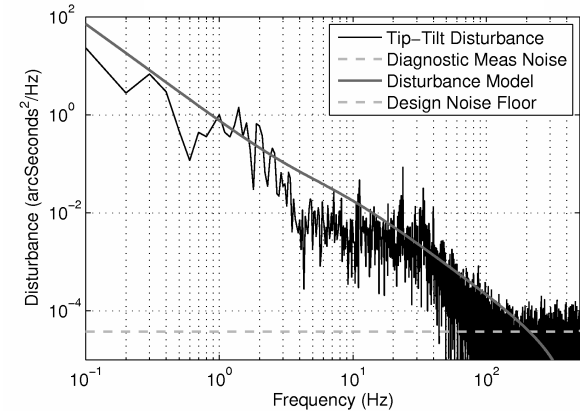

Figure 7. Disturbance model and noise PSDs for a bright guidestar.

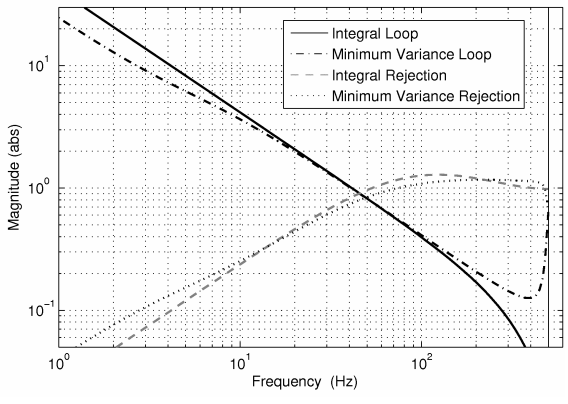

Figure 8. Loop and rejection transfer functions for feedback systems using the integral or minimum variance compensators.

Bode magnitude diagrams of the loop transfer function and rejection transfer function for the feedback systems using the integral compensator Eq. (12) and minimum variance compensator Eq. (13) are shown in Figure 8. The feedback loop using the minimum variance compensator rejects less disturbance power at low frequencies, but has a higher rejection bandwidth. The loop bandwidths are essentially the same. The increase in rejection bandwidth is reflected in the higher phase margin of the minimum variance loop (83.8˚ versus 72.5˚).

4.2 Medium Guidestar

Table 2. Performance using a medium guidestar.

	Integral Controller	**Minimum Variance Controller**
Residual RMS	279.8 nm	272.6 nm
Rejection Bandwidth	17 Hz	32 Hz
Phase Margin	88.1˚	100˚

The minimum variance compensator produces a 2.6% smaller residual variance than the integral compensator (see Table 2). The integral compensator that produces the minimum residual RMS is:

$$K_I(z) = 0.0281\frac{z}{z-1} \tag{14}$$

The minimum variance compensator again uses a disturbance model given by Eq. (11). The coloring filter gain that result in a minimum residual RMS is $g_a = 0.0116$ (see Figure 9). The resulting minimum variance compensator is:

$$K_{MV}(z) = 0.0577\left(\frac{z}{z-1}\right)\left(\frac{z}{z+0.70}\right)\left(\frac{z-0.972}{z-0.957}\right) \tag{15}$$

Note that again the minimum variance compensator consists of an integral element with two lead filters. One lead filter incorporates the model of the disturbance. The other lead filter compensates for the loop delay. Now, however, the lead is not as aggressive and has effect at a lower frequency.

Bode magnitude diagrams of the loop transfer function and rejection transfer function for the feedback systems using the integral compensator Eq. (14) and minimum variance compensator Eq. (15) are shown in Figure 10. The feedback loop using the minimum variance compensator rejects less disturbance power at low frequencies, but has a higher rejection bandwidth (although the amount of rejection is small). The loop bandwidths are essentially the same. The increase in rejection bandwidth is reflected in the higher phase margin of the minimum variance loop.

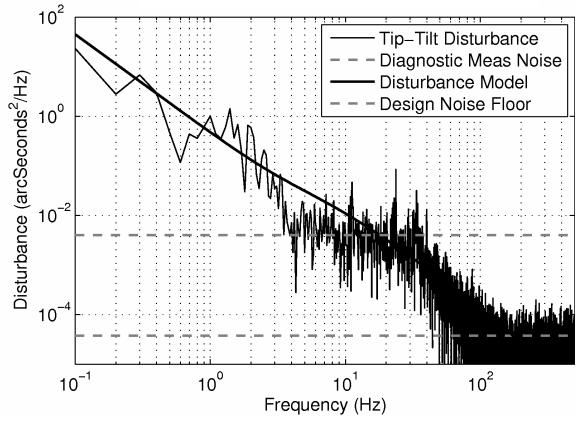

Figure 9. Disturbance model and noise PSDs for a medium guidestar.

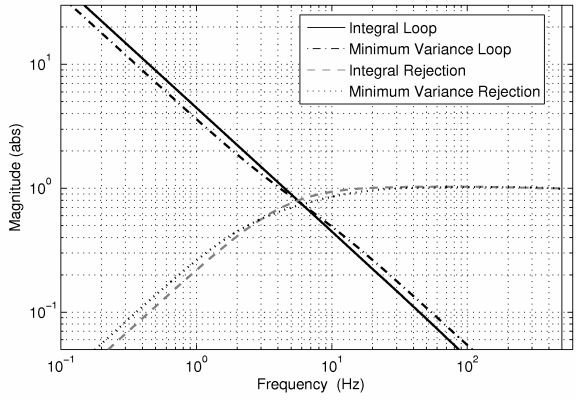

Figure 10. Loop and rejection transfer functions for feedback systems using the integral or minimum variance compensators.

4.3 Faint Guidestar

Table 3. Performance using a faint guidestar.

	Integral Controller	Minimum Variance Controller
Residual RMS	483.1 nm	481.8 nm
Rejection Bandwidth	8.5 Hz	10.5 Hz
Phase Margin	89.5°	89.7°

The minimum variance compensator produces a 0.3% smaller residual variance than the integral compensator (see Table 3). The integral compensator that produces the minimum residual RMS is:

$$K_I(z) = 0.0667\frac{z}{z-1} \tag{16}$$

The minimum variance compensator uses a 1st order integral disturbance model Eq. ((10) with $\alpha = \beta$). The coloring filter gain that result in a minimum residual RMS is $g_a = 0.0077$ (see Figure 11). The resulting minimum variance compensator is:

$$K_{MV}(z) = 0.0112\left(\frac{z}{z-1}\right)\left(\frac{z}{z+0.67}\right) \tag{17}$$

Note that the minimum variance compensator now consists of an integral element with one lead filter that compensates for the loop delay.

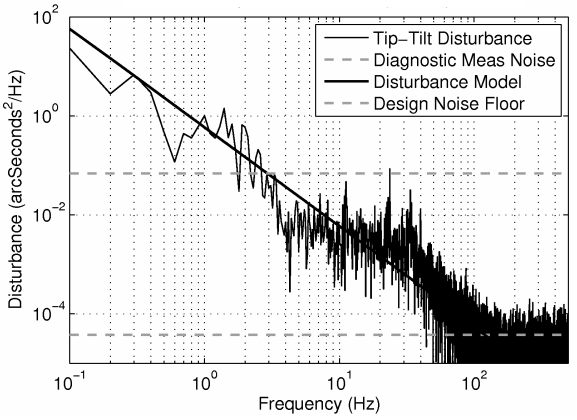

Figure 11. Disturbance model and noise PSDs for a bright guidestar.

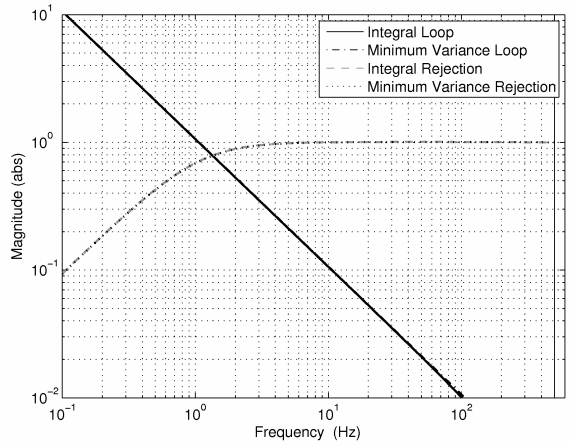

Figure 12. Loop and rejection transfer functions for feedback systems using the integral or minimum variance compensators.

Bode magnitude diagrams of the loop transfer function and rejection transfer function for the feedback systems using the integral compensator Eq. (16) and minimum variance compensator Eq. (17) are shown in Figure 12. The feedback loop using the minimum variance compensator is virtually the same as that using the integral compensator.

5. SUMMARY

The minimum variance compensator can improve the performance of an adaptive optics loop under certain conditions. The minimum variance controller explicitly compensates for the wavefront integration and sampling process. It can also take advantage of the frequency dependence of the PSD of the disturbance beyond the f^{-2} behavior that is implicitly assumed by the integral controller. To exhibit these potential advantages, these phenomena must have a significant effect on the residual variance.

This is illustrated by the comparison of the two controllers in Section 4. The rejection bandwidth is a significant fraction of the Nyquist frequency (approximately 20%). The additional lead provided by the minimum variance compensator in this frequency range allows the residual RMS to be reduced. The potential for improved residual RMS that can be obtained by compensating for the sampling process becomes less as the rejection bandwidth is reduced, as illustrated by the medium and faint guidestars.

The disturbance PSDs for the bright and medium guidestars show significant differences from the base f^{-2} dependence over the rejection frequency range. This shape can be exploited by the minimum variance controller by incorporating a model of this behavior in the compensator. For the faint guidestar, a f^{-2} model is a good description of the disturbance power to be rejected.

In summary, the minimum variance controller can improve adaptive optics system performance. The improvement increases as the guidestar becomes brighter, or as the shape of the disturbance PSD increasingly differs from the f^{-2} dependence. However, there is no performance improvement for faint guidestars with the PSD from Figure 4. This is because the integral controller is very nearly the minimum variance controller at low bandwidths (the effect of sampling is negligible) when for the f^{-2} behavior approximates the PSD up to the system bandwidth.

ACKNOWLEDGEMENTS

This work has been supported by the National Science Foundation Science and Technology Center for Adaptive Optics, managed by the University of California at Santa Cruz under cooperative agreement No. AST - 9876783.

REFERENCES

1. P. L. Wizinowich *et. al.*, "The W.M. Keck Laser Guide Star Adaptive Optics System: Overview," *Publications of the Astronomical Society of the Pacific*, **118**, p. 297-309, 2006.
2. M. A. van Dam, D. Le Mignant, and B. Macintosh, "Performance of the Keck Observatory Adaptive Optics System," *Applied Optics*, **43**, p. 5458-5467, 2004.
3. M. A. van Dam *et. al.*, "The W.M. Keck Laser Guide Star Adaptive Optics System: Performance Characterization," *Publications of the Astronomical Society of the Pacific*, **118**, p. 310-318, 2006.
4. J. W. Hardy, *Adaptive Optics for Astronomical Telescopes*, Oxford, New York, 1998.
5. D. P. Looze, "Minimum Variance Control Structure for Adaptive Optics Systems," *JOSA A*, **23**, p. 603-612, 2006.
6. P. D. Welch, "The use of the FFT for estimation of power spectra: a metod based on averaging over short, modified periodograms," *IEEE Trans. Audio and Acoustics*, **15**, p. 70-73, 1967.
7. D. P. Looze, "Realization of systems with CCD-based measurements," *Automatica*, **41**, pp. 2005-2009, 2005.
8. P. E. Gill, W. Murray, and M. H. Wright, *Practical Optimization*, Academic Press, New York, 1981.